J. Fluid Mech. (2001), *vol.* 437, *pp.* 121–142. Printed in the United Kingdom

Baroclinic topographic modons

By GREGORY M. REZNIK[1] AND GEORGI G. SUTYRIN[2]

[1]P. P. Shirshov Institute of Oceanology, 23 Krasikova Street, Moscow, 117256 Russia

[2]Graduate School of Oceanography, University of Rhode Island, Narragansett, RI 02882, USA

(Received 8 November 1999 and in revised form 15 October 2000)

The theory of solitary topographic Rossby waves (modons) in a uniformly rotating two-layer ocean over a constant slope is developed. The modon is described by an exact, form-preserving, uniformly translating, horizontally localized, nonlinear solution to the inviscid quasi-geostrophic equations. Baroclinic topographic modons are found to translate steadily along contours of constant depth in both directions: either with negative speed (within the range of the phase velocities of linear topographic waves) or with positive speed (outside the range of the phase velocities of linear topographic waves). The lack of resonant wave radiation in the first case is due to the orthogonality of the flow field in the modon exterior to the linear topographic wave field propagating with the modon translation speed, that is impossible for barotropic modons. Another important property of a baroclinic topographic modon is that its integral angular momentum must be zero only in the bottom layer; the total angular momentum can be non-zero unlike for the beta-plane modons over flat bottom. This feature allows modon solutions superimposed by intense monopolar vortices in the surface layer to exist. Explicit analytical solutions for the baroclinic topographic modons with piecewise linear dependence of the potential vorticity on the streamfunction are presented and analysed.

1. Introduction

Interest in the quasi-geostrophic solitary Rossby waves (so-called modons) is motivated by the important role of the long-lived large-scale coherent vortical structures in the dynamics of the oceans and atmospheres of the Earth and other planets. In the ocean these are rings, inthrathermocline lenses, and mesoscale eddies of the open ocean (e.g. Kamenkovich, Koshlyakovich & Monin 1986). In the atmosphere these are long-lived blocking events determining the weather over vast regions (e.g. McWilliams 1980). The well-known examples of such structures are large intense eddies in the atmosphere of Jupiter and other giant planets (e.g. Nezlin & Sutyrin 1994).

The problem of the resistance of such long-lived structures to Rossby wave dispersion stimulated theoretical studies of form-preserving, horizontally localized, nonlinear solutions to the equations of rotating fluids. A stationary barotropic solution was described by Stern (1975) who introduced the term 'modon', and steadily translating barotropic solutions were suggested by Larichev & Reznik (1976). On the flat beta-plane, the basic modon solution represents a dipolar vortex pair with a characteristic north–south antisymmetry. These dipoles propagate eastward at any speed, or westward at speeds greater than the long-wave speed. It is the nonlinear vortex pair interaction that allows the modon translation speed to be outside the range of linear Rossby waves to avoid resonant radiation.

Theoretical studies of modons have been extended in a number of ways in the frameworks of both geophysical fluid dynamics and plasma physics. The stability of modons, their collisions, influence of various factors such as friction, stratification, bottom topography, etc. upon the modons, and some new modon solutions were investigated. Because large-scale eddies are typically near geostrophic balance, the quasi-geostrophic equations were primarily used in the most of the studies summarized by Flierl (1987).

In this paper we focus our attention on the mutual effects of topography and stratification on the modon dynamics. These factors along with the beta-effect play key roles in the dynamics of meso- and large-scale geophysical vortices. For example, they are especially important in the continental slope regions characterized by rather steep slope where topography can be more significant than the beta-effect.

Up to now the effects of topography and stratification on the modons have been studied separately. In barotropic uniformly rotating fluid with constant slope the solutions are the same as on the beta-plane with a flat bottom. Reznik (1985) found an explicit modon solution for the paraboloidal bottom resulting in a closed trajectory around a seamount, while Mied, Kirwan & Lindemann (1992) constructed a family of modons rotating steadily over isolated topographic features. Swaters (1986) calculated analytically the evolution of barotropic modons over a slowly varying bottom relief. The interaction of modons with topography having a wide range of scales has been examined numerically by Carnevale *et al.* (1988*a*, *b*). They found that the barotropic modons are generally quite robust and are able to propagate coherently for long periods of time over a moderately rough bottom and smoothly varying topography.

Modon solutions in a stratified ocean with a flat bottom have also been constructed in a number of papers. Berestov (1979) found a three-dimensional modon in an unbounded continuously stratified ocean. Flierl *et al.* (1980, referred to herein as FLMR) analysed a wide variety of modons in a two-layer ocean and discovered that radially symmetric perturbations (so-called riders) of a special form but arbitrary amplitude can be superimposed on the basic solutions. Kizner (1984, 1986, 1988, 1997) investigated the modons with riders in a stratified ocean. All modons on the beta-plane as well as barotropic topographic modons have zero net angular momentum and the translation speed is outside the range of linear Rossby waves (except westward propagating modons with a baroclinic exterior found by FLMR).

Recently we have described some general properties of baroclinic topographic modons (BTMs) which distinguish them from other modons (Reznik & Sutyrin 2000). In this paper we focus on the cooperative effect of the topography and stratification on the modon dynamics and construct various BTM solutions. The paper is organized as follows. In § 2 the model is formulated; for simplicity we consider the quasi-geostrophic model of a uniformly rotating two-layer ocean with constant bottom slope. Section 3 contains a brief description of linear wave modes. General properties of the BTMs are considered in § 4. Equations for the BTMs with a piecewise-linear dependence of the potential vorticity on the streamlines are derived in § 5. In § 6 the solution is given for 'anomalously propagating' BTMs with negative translation speed within the range of the phase velocities of the linear topographic waves. The structure of such unusual BTMs and the dispersion relation between their size and propagation speed are analysed for the gravest modes. 'Traditional' modons with positive translation speed outside that range are described in § 7. It is shown that such a BTM can have superimposed on it an axisymmetric rider representing the monopolar vortex in the upper layer with non-zero net angular momentum. The

rider amplitude is arbitrary, thus the dipolar structure may to some extent be masked. A summary and discussion are given in § 8.

2. The model formulation

We consider a two-layer ocean rotating with a constant angular velocity $f_0/2$ over a sloping bottom. Assuming the bottom slope to be sufficiently small so that the fluid depth varies weakly on the motion scale, we use the quasi-geostrophic equations which are expressed in the form of conservation of potential vorticity in each layer:

$$\frac{\partial q_1}{\partial t} + J(\Psi_1, q_1) = 0, \tag{2.1a}$$

$$\frac{\partial q_2}{\partial t} + J(\Psi_2, q_2) + \beta_T \frac{\partial \Psi_2}{\partial x} = 0, \quad \beta_T = \frac{f_0}{\bar{h}_2} s. \tag{2.1b}$$

Here Ψ_1, Ψ_2 are the streamfunctions, subscripts 1, 2 correspond to the upper and lower layers, respectively, s is the constant bottom slope. J is the Jacobian; the fluid potential vorticities q_1, q_2 are given by the expressions

$$q_1 = \nabla^2 \Psi_1 + \frac{f_0^2}{g' \bar{h}_1}(\Psi_2 - \Psi_1), \quad q_2 = \nabla^2 \Psi_2 + \frac{f_0^2}{g' \bar{h}_2}(\Psi_1 - \Psi_2), \tag{2.2}$$

where $\bar{h}_1, \bar{h}_2$ are the constant mean depths of the layers, and g' the reduced gravity. The x-axis points along the slope and the y-axis across the slope in the direction of decreasing depth. Thus, without loss of generality the bottom slope s is assumed to be positive.

Introducing the length scale L using the internal Rossby scale for the lower layer,

$$L = \frac{\sqrt{g' \bar{h}_2}}{f_0}, \tag{2.3}$$

and

$$T^* = \frac{1}{\beta_T L} \equiv \frac{1}{s} \sqrt{\frac{\bar{h}_2}{g'}}, \quad U^* = \beta_T L^2 \equiv \frac{g' s}{f_0} \tag{2.4}$$

as the time and velocity scales, respectively, we write (2.1)–(2.2) in the non-dimensional form

$$\frac{\partial q_1}{\partial t} + J(\Psi_1, q_1) = 0, \quad \frac{\partial q_2}{\partial t} + J(\Psi_2, q_2) + \frac{\partial \Psi_2}{\partial x} = 0, \tag{2.5a, b}$$

$$q_1 = \nabla^2 \Psi_1 + b(\Psi_2 - \Psi_1), \quad q_2 = \nabla^2 \Psi_2 + (\Psi_1 - \Psi_2), \quad b = \bar{h}_2 / \bar{h}_1. \tag{2.6a, b}$$

Two types of stationary solutions exist for the system (2.5)–(2.6), similar to solutions on the beta-plane with a flat bottom:

(i) arbitrary zonal flows

$$\Psi_i = \Psi_i(y), \quad i = 1, 2; \tag{2.7}$$

(ii) horizontally localized form-preserving vortices steadily propagating along the slope with the speed U, i.e.

$$\Psi_i = \Psi_i(x - Ut, y), \quad i = 1, 2. \tag{2.8}$$

Modons represent the solutions (2.8) for (2.5) written in moving coordinates:

$$-U \frac{\partial q_1}{\partial x} + J(\Psi_1, q_1) = 0, \quad -U \frac{\partial q_2}{\partial x} + J(\Psi_2, q_2) + \frac{\partial \Psi_2}{\partial x} = 0 \tag{2.9a, b}$$

In particular, a stationary vortex in the upper layer and zero velocity in the lower layer satisfies (2.9):

$$U = 0, \quad J(\Psi_1, \nabla^2\Psi_1) = 0, \quad \Psi_2 = 0. \tag{2.10a,b,c}$$

An important example of the state (2.10) is the radially symmetric vortex

$$\Psi_1 = \Psi_1(r), \quad \Psi_2 = 0, \tag{2.11a,b}$$

where $\Psi_1(r)$ is an arbitrary function.

Obviously the upper-layer vortex that obeys (2.10) cannot remain stationary if the beta-effect is taken into consideration because of the Rossby wave radiation.

3. Linear modes

First we consider the linear waves

$$\Psi_n = \Psi_n^w = A_n \exp\left[\mathrm{i}(kx + ly - \omega t)\right], \quad n = 1, 2, \tag{3.1a}$$

satisfying the linearized version of (2.5)–(2.6). The waves obey the following dispersion relation:

$$\omega = \frac{k}{\kappa^2}\frac{\kappa^2 + b}{\kappa^2 + 1 + b}, \quad \boldsymbol{\kappa} = (k, l), \tag{3.1b}$$

and the amplitude ratio

$$A_1 = \frac{b}{\kappa^2 + b}A_2. \tag{3.1c}$$

From (3.1b) we see that the x-component U of the wave phase velocity is always negative,

$$U = \frac{\omega}{k} = -\frac{\kappa^2 + b}{\kappa^2(\kappa^2 + 1 + b)} < 0, \tag{3.2}$$

thus the waves propagate so that the deeper water is to the left of the wavevector. The velocity U changes between $-\infty$ for $\kappa \to 0$ and 0 for $\kappa \to \infty$, similarly to the barotropic Rossby waves.

The topographic waves (3.1) are intensified in the bottom layer, especially in the limit of the bottom reduced-gravity model ($\kappa^2 \gg b$ for short waves or when $\bar{h}_1 \gg \bar{h}_2$). In another limit ($\kappa^2 \ll b$ for long waves or when $\bar{h}_2 \gg \bar{h}_1$), the wave amplitude does not depend on the depth and the wave (3.1) is nearly the barotropic Rossby wave with $\beta = \beta_T$.

It should be noted that the topographic wave radiation does not affect the upper-layer potential vorticity because the potential vorticity perturbations are zero in the upper layer for waves (3.1). Therefore, an arbitrary solution of the linearized system (2.5)–(2.6) with a non-zero initial upper-layer potential vorticity q_1 approaches with time the state (2.10) due to dispersion of potential vorticity in the lower layer. For example, an axisymmetric perturbation confined initially to the *lower* layer produces the axisymmetric vortex (2.11) concentrated in the *upper* layer as $t \to \infty$ (see Reznik 1999 for details).

4. General properties of baroclinic topographic modons

Here we derive some general properties of the BTMs from (2.9) which can be written in the form

$$J(\Psi_1 + Uy, q_1) = 0, \quad J(\Psi_2 + Uy, q_2 + y) = 0. \tag{4.1a,b}$$

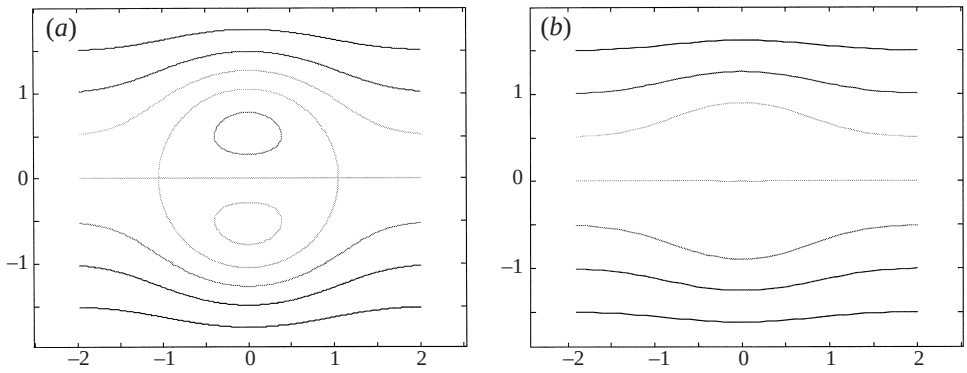

FIGURE 1. Schematical pattern of the modon streamlines for the upper (*a*) and lower (*b*) layers in moving coordinates.

These equations have the first integrals

$$q_1 = S_1(\Psi_1 + Uy), \quad q_2 = S_2(\Psi_2 + Uy) - y, \tag{4.2a,b}$$

where $S_1(z), S_2(z)$ are some differentiable functions.

At the open streamlines $\Psi_i + Uy = \text{const}$, $i = 1, 2$, which become straight lines $y = \text{const}$ far from the modon centre, taking $x \to \pm\infty$ in (4.2) we obtain

$$S_1(z) = 0, \quad S_2(z) = \frac{1}{U} z. \tag{4.3a,b}$$

Thus, along the open streamlines (4.2) take the form

$$\nabla^2 \Psi_1 + b(\Psi_2 - \Psi_1) = 0, \quad \nabla^2 \Psi_2 + (\Psi_1 - \Psi_2) - \frac{1}{U} \Psi_2 = 0. \tag{4.4a,b}$$

One can readily show that the linear system (4.4) does not possess non-singular localized solutions. Therefore, the streamline pattern must contain at least one domain with closed streamlines and the vorticity distribution within such a domain differs from (4.3). The streamline pattern is shown schematically in figure 1. The domains with open and closed streamlines will be referred to as exterior and interior domains, respectively; and the streamline Γ as the separating streamline.

4.1. *Exterior domain*

In the exterior domain the motion is described by the system (4.4) which can be written in terms of the normal modes

$$\tilde{\Psi}_1 = \Psi_1 + \alpha_1 \Psi_2, \quad \tilde{\Psi}_2 = \Psi_1 + \alpha_2 \Psi_2 \tag{4.5a,b}$$

'decoupling' the equations (4.4*a*, *b*) so that

$$\nabla^2 \tilde{\Psi}_1 - p_1^2 \tilde{\Psi}_1 = 0, \quad \nabla^2 \tilde{\Psi}_2 - p_2^2 \tilde{\Psi}_2 = 0. \tag{4.6a,b}$$

The mode parameters α_j and p_j are related as follows:

$$p^2 = b - \alpha = 1 + 1/U - b/\alpha \tag{4.7}$$

so that

$$\alpha_1 = -m + \sqrt{m^2 + b}, \quad \alpha_2 = -m - \sqrt{m^2 + b}, \quad m = \tfrac{1}{2}(1 - b + 1/U). \tag{4.8a,b,c}$$

From (4.7)–(4.8) we see that

$$\alpha_1 > 0, \quad \alpha_2 < 0 \tag{4.9}$$

and

$$p_1^2 < 0, \quad p_2^2 > 0 \quad \text{for} \quad U < 0, \tag{4.10a}$$

$$p_1^2 > 0, \quad p_2^2 > 0 \quad \text{for} \quad U > 0. \tag{4.10b}$$

Localized solutions to the equations (4.6) may exist only for $p_j^2 > 0$, thus from (4.10*a*) we see that the first normal mode must be zero in the exterior of the modon moving with the negative speed U,

$$\tilde{\Psi}_1 = \Psi_1 + \alpha_1 \Psi_2 = 0, \quad \tilde{\Psi}_2 = \Psi_1 + \alpha_2 \Psi_2 \neq 0. \tag{4.11a,b}$$

To understand the physical meaning of the condition (4.11) we consider the harmonic wave (3.1) propagating with the same velocity $U < 0$. Obviously, (4.4)–(4.9) are also valid for this wave. However, contrary to the modon case, for the harmonic solution to the equation (4.6*a*) with $p_1^2 < 0$, the second normal mode must be zero:

$$\tilde{\Psi}_1 = \Psi_1 + \alpha_1 \Psi_2 \neq 0, \quad \tilde{\Psi}_2 = \Psi_1 + \alpha_2 \Psi_2 = 0. \tag{4.12a,b}$$

Comparing (4.11) to (4.12) we see that the external streamfunction field of the modon moving with the 'resonance' negative translation speed $U < 0$ is *orthogonal* to the streamfunction of the harmonic wave propagating with the same velocity.† It is this orthogonality that allows the modon to not excite any harmonic waves and to be localized. We emphasize that the conditions (4.11) are applied only in the exterior domain; in the modon interior they are not valid (see § 5). One can say that resonant radiation produced by the resonant component within the modon core is suppressed by the nonlinear effects. The analogous property was also found for the Rossby modon with baroclinic exterior in a two-layer ocean of constant depth (FLMR).

The solution in the exterior depends on the sign of U. If $U < 0$ then we have form (4.5), (4.6), (4.11)

$$\Psi_1 = -\frac{\alpha_1}{\alpha_2 - \alpha_1}\tilde{\Psi}_2, \quad \Psi_2 = \frac{1}{\alpha_2 - \alpha_1}\tilde{\Psi}_2, \tag{4.13a,b}$$

where

$$\tilde{\Psi}_2 = \sum_{n=1}^{\infty} K_n(p_2 r)(C_{2n}\cos n\theta + D_{2n}\sin n\theta). \tag{4.14}$$

Here and below $K_n(z)$, $I_n(z)$ are the modified Bessel functions, and $J_n(z)$ the Bessel functions; r, θ are polar coordinates with their origin at the vortex centre.

For $U > 0$ both normal modes $\tilde{\Psi}_1, \tilde{\Psi}_2$ can be non-zero and the exterior solution is written as

$$\Psi_1 = \frac{1}{\alpha_2 - \alpha_1}(\alpha_2\tilde{\Psi}_1 - \alpha_1\tilde{\Psi}_2), \quad \Psi_2 = \frac{1}{\alpha_2 - \alpha_1}(\tilde{\Psi}_2 - \tilde{\Psi}_1), \tag{4.15a,b}$$

where

$$\tilde{\Psi}_j = \sum_{n=1}^{\infty} K_n(p_j r)(C_{jn}\cos n\theta + D_{jn}\sin n\theta), \quad j = 1, 2. \tag{4.16}$$

† The scalar production of the fields $\boldsymbol{P} = \begin{pmatrix} P_1 \\ P_2 \end{pmatrix}$, $\boldsymbol{Q} = \begin{pmatrix} Q_1 \\ Q_2 \end{pmatrix}$ is defined here as $\boldsymbol{P} \cdot \boldsymbol{Q} = h_1 P_1 Q_1 + h_2 P_2 Q_2$.

4.2. *Angular momentum*

To analyse the angular momentum, we consider the localized solution to (2.5)–(2.6) decaying faster than r^{-2} for $r \to \infty$. Multiplying (2.5) by x and integrating the resulting equations throughout the plane we obtain after simple transformations

$$\int \Psi_2 \,\mathrm{d}x\,\mathrm{d}y = 0, \quad \frac{\partial}{\partial t}\int x(\Psi_2 - \Psi_1)\,\mathrm{d}x\,\mathrm{d}y + \int xJ(\Psi_1, \Psi_2)\,\mathrm{d}x\,\mathrm{d}y = 0. \qquad (4.17a, b)$$

The equations (4.17) are the necessary conditions for the existence of the localized vortices in the two-layer ocean with a sloping bottom. Thus, only the *lower* layer vortex has a zero angular momentum, whereas the total angular momentum of the localized vortex can be non-zero and the upper layer vortex can be a monopole. We emphasize that these conditions are substantially different from the analogous conditions on the beta-plane where the total angular momentum of the localized vortex must be zero (Flierl *et al.* 1983). For the modon the condition (4.17*b*) is given by

$$\int \Psi_1 \,\mathrm{d}x\,\mathrm{d}y = \frac{1}{U}\int xJ(\Psi_1, \Psi_2)\,\mathrm{d}x\,\mathrm{d}y. \qquad (4.18)$$

5. Modons with linear interior vorticity distributions S_1, S_2

5.1. *Interior solution*

Following Larichev & Reznik (1976) and FLMR we assume that the interior domains are circles of the same radius a with the linear vorticity distributions S_1, S_2:

$$S_i(z) = s_i z + Q_i, \quad i = 1, 2, \qquad (5.1)$$

where the coefficients s_i, Q_i are determined from the matching conditions at the separating streamlines $r = a$.

Note that the separating streamlines need not have either the same radius or the same centre, but such assumptions were made in the most of previous studies of modons in order to facilitate analytical progress. A notable exception is the beta-pane study by Pakyri & Nycander (1996) in which circular streamlines were offset a small distance from each other in the meridional direction, which then allows a 'hetonic' propagation mechanism to become important.

We now substitute (5.1) into (4.2) and introduce the normal modes

$$T_j = \Psi_1 + \gamma_j \Psi_2, \quad j = 1, 2, \qquad (5.2)$$

that satisfy the equation

$$\nabla^2 T_j + k_j^2 T_j = -[(1 + \gamma_j)k_j^2 U + \gamma_j]y + Q_1 + \gamma_j Q_2; \qquad (5.3)$$

the parameters k_j, γ_j are related as follows:

$$k^2 = \gamma - s_1 - b = \frac{b}{\gamma} - s_2 - 1 \qquad (5.4)$$

The solution to (5.3) can be written in the form

$$T_j = \sum_{n=0}^{\infty} J_n(k_j r)(A_{jn}\cos n\theta + B_{jn}\sin n\theta) - \frac{Q_1 + \gamma_j Q_2}{k_j^2} - \frac{(1 + \gamma_j)k_j^2 U + \gamma_j}{k_j^2} r\sin\theta,$$
$$j = 1, 2, \quad (5.5)$$

where

$$J_n = I_n(k_j r) \quad \text{for} \quad k_j^2 < 0. \tag{5.6}$$

The interior solution is expressed by the normal modes in the form

$$\Psi_1 = \frac{1}{\gamma_2 - \gamma_1}(\gamma_2 T_1 - \gamma_1 T_2), \quad \Psi_2 = \frac{1}{\gamma_2 - \gamma_1}(T_2 - T_1). \tag{5.7a,b}$$

5.2. *Conditions at the separating streamline $r = a$*

We require the continuity of the functions Ψ_i and their derivatives at the separating streamline:

$$\Psi_i\big|_{r=a-0} = \Psi_i\big|_{r=a+0}, \quad \left.\frac{\partial \Psi_i}{\partial r}\right|_{r=a-0} = \left.\frac{\partial \Psi_i}{\partial r}\right|_{r=a+0}, \quad i = 1, 2. \tag{5.8a,b}$$

In addition to (5.8) one has to take into account that the circle $r = a$ is a streamline $\Psi_i + Uy = C_i = \text{const}$, i.e.

$$\Psi_i\big|_{r=a\pm 0} = -Ua \sin\theta + C_i, \quad i = 1, 2. \tag{5.9}$$

Obviously the conditions (5.8), (5.9) are not independent and it is sufficient to choose the condition

$$\Psi_i\big|_{r=a+0} = -Ua \sin\theta + C_i, \quad i = 1, 2. \tag{5.10}$$

instead of (5.9).

Conditions (5.8)–(5.10) are written assuming that the interior domains exist in both the layers. If the interior domain is absent, for example, in the lower layer then the condition (5.10) for $i = 2$ should be omitted.

Substitution of (4.15), (4.16) and (5.5), (5.7) into (5.8), (5.10) gives an infinite set of linear equations for the coefficients $A_{jn}, B_{jn}, C_{jn}, D_{jn}$. This system is greatly simplified by the fact that for any fixed m the equations relating the parameters A_{jm} and C_{jm} and the equations relating B_{jm} and D_{jm} depend neither on each other nor on the parameters A_{jk}, B_{jk}, C_{jk}, D_{jk} for $k \neq m$. Moreover, the equations for these parameters are homogeneous except the equations for A_{j0}, C_{j0}, B_{j1}, and D_{j1}. Therefore, in what follows we assume

$$\left.\begin{aligned} A_{jk} = C_{jk} = 0 \quad &\text{for} \quad k \neq 0, \\ B_{jk} = D_{jk} = 0 \quad &\text{for} \quad k \neq 1. \end{aligned}\right\} \tag{5.11}$$

In other words, only the axisymmetric component and the dipole proportional to $\sin\theta$ remain non-zero in the expansions (4.16), (5.5):

$$\tilde{\Psi}_j = C_{j0} K_0(p_j r) + D_{j1} K_1(p_j r) \sin\theta, \quad j = 1, 2, \tag{5.12a}$$

$$T_j = A_{j0} J_0(k_j r) + B_{j1} J_1(k_j r) \sin\theta + \frac{Q_1 + \gamma_j Q_2}{k_j^2} - \frac{(1 + \gamma_j) k_j^2 U + \gamma_j}{k_j^2} r \sin\theta, \quad j = 1, 2. \tag{5.12b}$$

The streamfunctions in the layers are represented as

$$\Psi_i = \Psi_i^{(r)}(r) + \Psi_i^{(d)}, \quad \Psi_i^{(d)} = \Phi_i(r) \sin\theta, \quad i = 1, 2. \tag{5.13a,b}$$

The dipole component $\Psi_i^{(d)}$ and the axisymmetric component $\Psi_i^{(r)}$ will be referred to as the dipole modon and the rider, respectively.

The equations determining the dipole modon $\Psi_i^{(d)}$ and relations between parameters D_{j1}, B_{j1}, U, a, and k_j (see below) do not depend on the parameters $A_{j0}, C_{j0}, Q_1, Q_2, C_1, C_2$ determining the rider. If Q_1, Q_2 are zero in (5.1) and $C_i = 0$ in (5.10) then the rider component $\Psi_i^{(r)}$ in (5.13*a*) vanishes and the solitary wave is reduced to the dipole modon. Therefore the dipole modon (if any) exists independent of the rider; namely the dipole component $\Psi_i^{(d)}$ is the 'engine' forcing the solitary wave to move along the x-axis. One can readily also check that the conditions (5.8), (5.10) provide the continuity of the dipole modon up to the second derivatives.

6. Modons with negative translation speed

In the case $U < 0$ the exterior normal modes (5.12*a*) are represented as

$$\tilde{\Psi}_1 = 0, \quad \tilde{\Psi}_2 = C_{20}K_0(p_2 r) + D_{21}K_1(p_2 r) = \sin\theta. \tag{6.1a,b}$$

If the interior domains with the linear dependence (5.1) are the same in both layers, one can readily check that the matching conditions (5.10) cannot be satisfied with (4.13) and (6.1). Therefore, modons with negative translation speed and interior domains in both layers may exist only if the interior domains in the upper and lower layers are not the same as each other (cf. FLMR). Here we consider for simplicity the case when the interior domain is absent in the lower layer, i.e. the exterior dependence (4.3*b*) is valid throughout the lower layer and therefore in (5.1)

$$Q_2 = 0, \quad s_2 = 1/U. \tag{6.2a,b}$$

Then the lower-layer dynamics obey (4.4*b*) while the relations (5.4) take the form

$$k^2 = \gamma - s_1 - b = \frac{b}{\gamma} - \frac{1}{U} - 1. \tag{6.3}$$

We now substitute the solutions (4.13), (5.7) into the conditions (5.8) and (5.10) for $i = 1$. For the dipole modon we obtain after some algebra

$$D_{21} = \frac{\alpha_2 - \alpha_1}{\alpha_1}\frac{Ua}{K_1(p_2 a)}, \tag{6.4a}$$

$$B_{j1}J_1(k_j a) - \frac{(1+\gamma_j)k_j^2 U + \gamma_j}{k_j^2}a = \frac{\gamma_j - \alpha_1}{\alpha_2 - \alpha_1}D_{21}K_1(p_2 a), \tag{6.4b}$$

$$B_{j1}\operatorname{sgn} k_j^2 |k_j| a J_2(k_j a) = \frac{\gamma_j - \alpha_1}{\alpha_2 - \alpha_1}D_{21}p_2 a K_2(p_2 a), \tag{6.4c}$$

where $j = 1, 2$. Five equations (6.4) for three coefficients B_{11}, B_{21}, and D_{21} have the two conditions of solvability:

$$\operatorname{sgn} k_j^2 \frac{J_1(k_j a)}{|k_j| a J_2(k_j a)} = \frac{K_1(p_2 a)}{p_2 a K_2(p_2 a)}\frac{\gamma_j[k_j^2(1+\alpha_1)U + \alpha_1]}{k_j^2 U(\gamma_j - \alpha_1)}. \tag{6.5}$$

Using (4.7), and (6.3) one can show that

$$\frac{\gamma_j[k_j^2(1+\alpha_1)U + \alpha_1]}{k_j^2 U(\gamma_j - \alpha_1)} = -\frac{p_2^2}{k_j^2}, \tag{6.6}$$

therefore (6.5) is simplified to

$$\frac{J_2(k_j a)}{|k_j| a J_1(k_j a)} = -\frac{K_2(p_2 a)}{p_2 a K_1(p_2 a)}, \quad j = 1, 2. \tag{6.7}$$

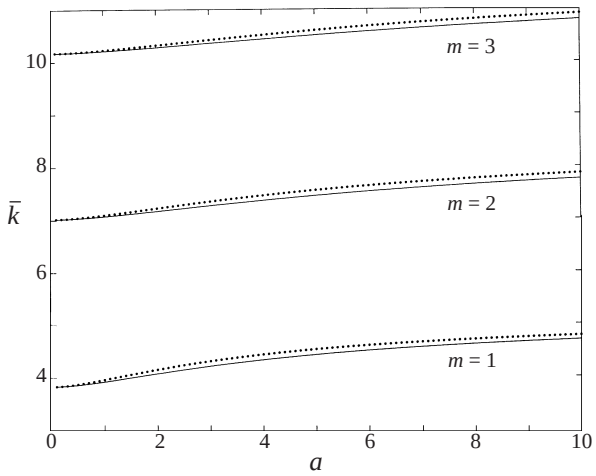

FIGURE 2. First three solutions of (6.7) for $b = 1$ and limiting values of $p_2 = 1$ (solid lines) and for $p_2 = (1 + \sqrt{5})/2$ (dotted lines).

If $k_j^2 < 0$ then $J_m(k_j a) = I_m(|k_j|a)$ and (6.7) cannot be satisfied. Hence, we have $k_j^2 > 0$ in (6.7). Equations (6.7) are exactly the same as the analogous equations for the Rossby modon with baroclinic exterior at the beta-plane discussed in FLMR. The parameter p_2 does not depend on a, and the right-hand side of (6.7) varies monotonically from $-\infty$ to 0 when the radius a increases from 0 to $+\infty$. Thus, a countable set of the roots $\bar{k}_m = k_m a$ of (6.7) exists within the range between the roots of J_1 and J_2. Any two of them have to obey the relation that simply follows from (6.3):

$$\left(\frac{\bar{k}_1^2}{a^2} + 1 + \frac{1}{U}\right)\left(\frac{\bar{k}_2^2}{a^2} + 1 + \frac{1}{U}\right) = -b. \tag{6.8}$$

For negative translation speed, solutions to (6.8) may exist only for $-1 < U < 0$, so that (4.7) provides the limits for the external parameter p_2:

$$b < p_2^2 < \tfrac{1}{2}(b + \sqrt{b^2 + 4b}). \tag{6.9}$$

The boundaries of the first three roots $\bar{k}_m(a)$ of (6.7) for limiting values (6.9) of p_2 are shown in figure 2 for the depth ratio $b = 1$.

The system (6.7), (6.8) consists of three equations for four parameters $\bar{k}_1, \bar{k}_2, U, a$. Therefore, for a fixed a, we can find two branches of U from (6.8), assuming $\bar{k}_1, \bar{k}_2$ are within the ranges shown in figure 2:

$$U_+ = \frac{2a^2}{2a^2 + (\bar{k}_1^2 + \bar{k}_2^2 + G)}, \quad U_- = \frac{2a^2}{2a^2 + (\bar{k}_1^2 + \bar{k}_2^2 - G)}, \tag{6.10}$$

where

$$G^2 = (\bar{k}_2^2 - \bar{k}_1^2)^2 - 4a^4 b. \tag{6.11}$$

Asymptotically for $a^2 \ll \bar{k}_1^2$ we obtain from (6.10), (6.11) $U_+ \approx -a^2/\bar{k}_2^2$, and $U_- \approx -a^2/\bar{k}_1^2$. These branches match each other at $a = a_{max}$ which can be estimated assuming $G^2 = 0$ in (6.11):

$$a_{max}^2 = \frac{1}{2\sqrt{b}}[(\bar{k}_2^2)_{max} - (\bar{k}_1^2)_{min}]. \tag{6.12}$$

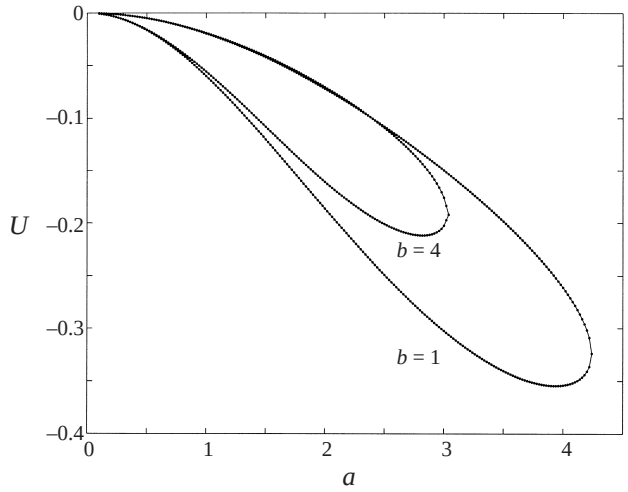

FIGURE 3. Modon with negative translation speed. Dependence of the propagation speed U on the modon radius a for limiting values of $p_2 = \sqrt{b}$ (solid lines) and $p_2(U_{max})$ (dotted lines) when $b = 1$ and $b = 4$.

The solutions (6.10) cease to exist for $a > a_{max}$. the existence of a maximum size for this kind of modon with negative translation speed is related to the maximum difference in the values of roots $(\bar{k}_2^2)_{max} - (\bar{k}_1^2)_{min}$ as seen in (6.12). Correspondingly, as one can find by estimating the minimum of (6.10), the modon propagation speed is limited by

$$U > -U_{max}, \quad U_{max} = \frac{a_{max}^2}{a_{max}^2 + (\bar{k}_2)_{min}(\bar{k}_1)_{min}}. \tag{6.13}$$

Thus, the boundaries of the branches given by (6.10) can be narrowed with $\bar{k}_1(a), \bar{k}_2(a)$ calculated from (6.7) with limiting values of $p_2 = \sqrt{b}$ and $p_2(U_{max})$. Figure 3 shows these boundaries for the dispersion relation $U(a)$ with the gravest roots $\bar{k}_1(a), \bar{k}_2(a)$ for different depth ratios. They visually coincide and one can see that both a_{max} and U_{max} decrease when b increases, in agreement with (6.12) and (6.13).

The streamline pattern in the lower layer is dominated by the first normal mode, T_1, which has a dipolar character with two vortex centres. In the upper layer the flow also has two vortex centres for the slower branch U_+ (figure 4), while the presence of the second normal mode, T_2, with four centres can be seen for the faster branch U_- (figure 5). The amplitude ratio $\max(|\Psi_2|)/\max(|\Psi_1|)$ increases with the modon size a.

The axisymmetric modon component (rider) is determined by four coefficients Q_1, A_{10}, A_{20}, and C_{20} satisfying four equations:

$$\frac{Q_1}{k_j^2} + A_{j0}J_0(k_j a) = \frac{\gamma_j - \alpha_1}{\alpha_2 - \alpha_1} C_{20}K_0(p_2 a), \tag{6.14a}$$

$$k_j A_{j0} J_1(k_j a) = \frac{p_2(\gamma_j - \alpha_1)}{\alpha_2 - \alpha_1} C_{20}K_1(p_2 a). \tag{6.14b}$$

The solvability condition for the homogeneous linear system (6.14) can be written as

$$k_1^2(\gamma_1 - \alpha_1)\left[\frac{J_0(k_1 a)}{k_1 J_1(k_1 a)} - \frac{K_0(p_2 a)}{p_2 K_1(p_2 a)}\right] = k_2^2(\gamma_2 - \alpha_1)\left[\frac{J_0(k_2 a)}{k_2 J_1(k_2 a)} - \frac{K_0(p_2 a)}{p_2 K_1(p_2 a)}\right]. \tag{6.15}$$

Using (4.7), (6.3), and (6.7) one can show that (6.15) is satisfied. Thus the axisym-

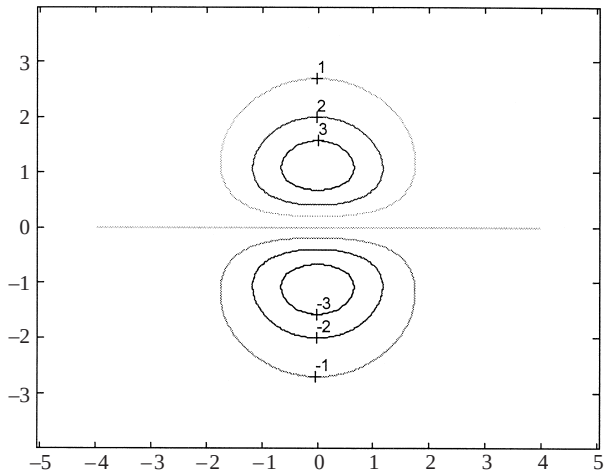

FIGURE 4. Modon with negative translation speed. An example of the upper layer dipole streamfunction $(-\Psi_1/U)$ for the slower branch U_+ when $a = \sqrt{2}$ and $b = 1$.

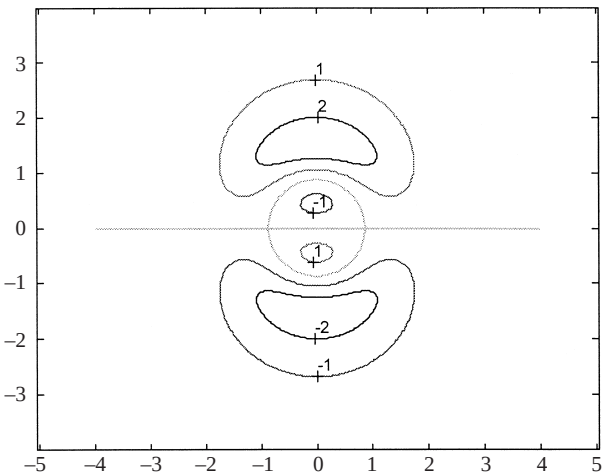

FIGURE 5. Modon with negative translation speed. An example of the upper layer streamfunction $(-\Psi_1/U)$ with four vortex centres for the faster branch U_- when $a = \sqrt{2}$ and $b = 1$.

metric rider exists and is determined by the axisymmetric parts of the fields (5.5), (5.7) and (4.15), (6.1) with the coefficients

$$A_{j0} = \frac{p_2(\gamma_j - \alpha_1)}{\alpha_2 - \alpha_1} \frac{K_1(p_2 a)}{k_j J_1(k_j a)} C_{20}, \tag{6.16a}$$

$$Q_1 = k_1^2 \frac{\gamma_1 - \alpha_1}{\alpha_2 - \alpha_1} \left[K_0(p_2 a) - \frac{p_2 K_1(p_2 a) J_0(k_1 a)}{k_j J_1(k_1 a)} \right] C_{20}. \tag{6.16b}$$

Here C_{20} (and therefore the rider amplitude) is arbitrary. The rider streamfunction is continuous, as are its first derivatives. Note, that the angular momentum of the rider constructed is zero in each layer due to the absence of the interior domain in the lower layer. To show this we integrate (4.4*b*) throughout the plane; from (4.17*a*)

we obtain

$$\int \Psi_1 \, \mathrm{d}x \, \mathrm{d}y = 0. \tag{6.17}$$

The same is valid when the interior domain is absent in the upper layer and (4.4*a*) is satisfied throughout the plane. In the next Section we show that the total angular momentum of a BTM possessing internal domains in both layers and moving with positive U can be non-zero.

7. Modons with positive translation speed

We now consider the modons moving with a positive translation speed $U > 0$ and possessing identical interior domains in both layers. The solution in this case is given by (4.15), (5.7) together with (5.12).

The conditions at the separating streamline for the dipole modon can be written as

$$\frac{1}{\alpha_2 - \alpha_1}[\alpha_2 D_{11} K_1(p_1 a) - \alpha_1 D_{21} K_1(p_2 a)] = -Ua, \tag{7.1a}$$

$$\frac{1}{\alpha_2 - \alpha_1}[D_{21} K_1(p_2 a) - D_{11} K_1(p_1 a)] = -Ua, \tag{7.1b}$$

$$B_{j1} J_1(k_j a) - \frac{(1+\gamma_j)k_j^2 U + \gamma_j}{k_j^2} a = \frac{1}{\alpha_2 - \alpha_1}[(\alpha_2 - \gamma_j) D_{11} K_1(p_1 a) + (\gamma_j - \alpha_1) D_{21} K_1(p_2 a)], \tag{7.1c}$$

$$B_{j1} \operatorname{sgn} k_j^2 |k_j| a J_2(k_j a) = \frac{1}{\alpha_2 - \alpha_1}[(\alpha_2 - \gamma_j) D_{11} p_1 a K_2(p_1 a) + (\gamma_j - \alpha_1) D_{21} p_2 a K_2(p_2 a)]. \tag{7.1d}$$

It readily follows from (7.1*a*, *b*, *c*) that

$$D_{11} = -(1+\alpha_1)\frac{Ua}{K_1(p_1 a)}, \quad D_{21} = -(1+\alpha_2)\frac{Ua}{K_1(p_2 a)}, \quad B_{j1} = \frac{\gamma_j a}{k_j^2 J_1(k_j a)}. \tag{7.2a, b, c}$$

Substituting (7.2) into (7.1*d*) we obtain after some algebra two conditions of solvability of the system (7.1):

$$\frac{J_2(k_j a)}{|k_j| J_1(k_j a)} = \frac{M(U,a)}{\gamma_j} + N(U,a), \quad j = 1, 2, \tag{7.3a}$$

where

$$M = \frac{U}{\alpha_1 - \alpha_2}\left[\alpha_2(1+\alpha_1)\frac{p_1 K_2(p_1 a)}{K_1(p_1 a)} - \alpha_1(1+\alpha_2)\frac{p_2 K_2(p_2 a)}{K_1(p_2 a)}\right], \tag{7.3b}$$

$$N = \frac{U}{\alpha_1 - \alpha_2}\left[(1+\alpha_2)\frac{p_2 K_2(p_2 a)}{K_1(p_2 a)} - (1+\alpha_1)\frac{p_1 K_2(p_1 a)}{K_1(p_1 a)}\right]. \tag{7.3c}$$

It is convenient to express γ_j in terms of k_j in (7.3*a*). To do this we use the following relations, which simply follow from (6.3):

$$k_1^2 - k_2^2 = \gamma_1 - \gamma_2, \quad \gamma_1 \gamma_2 = -b. \tag{7.4a, b}$$

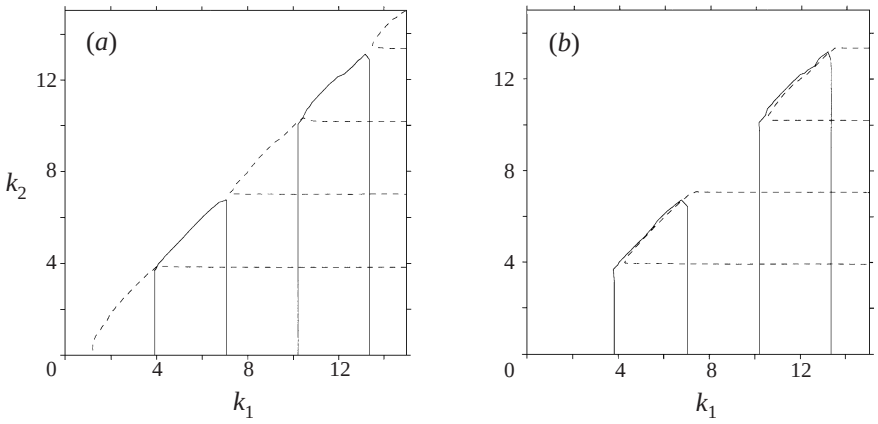

FIGURE 6. Modon with positive translation speed. Solid and dashed lines correspond to the equations (7.9*a*) and (7.9*b*), respectively for $U = a = 1$, and $b = 1$. The points of intersection are the roots k_1, k_2 of the system (7.9). (*a*) case 1, (*b*) case 2.

By virtue of (7.4) the pair of parameters γ_1, γ_2 can be expressed in terms of k_1, k_2 in two ways:

$$\gamma_1^{(1)} = \tfrac{1}{2}(k_1^2 - k_2^2) + \sqrt{\tfrac{1}{4}(k_1^2 - k_2^2)^2 - b}, \quad \gamma_2^{(1)} = -\tfrac{1}{2}(k_1^2 - k_2^2) + \sqrt{\tfrac{1}{4}(k_1^2 - k_2^2)^2 - b}, \tag{7.5a,b}$$

$$\gamma_1^{(2)} = \tfrac{1}{2}(k_1^2 - k_2^2) - \sqrt{\tfrac{1}{4}(k_1^2 - k_2^2)^2 - b}, \quad \gamma_2^{(2)} = -\tfrac{1}{2}(k_1^2 - k_2^2) - \sqrt{\tfrac{1}{4}(k_1^2 - k_2^2)^2 - b}. \tag{7.6a,b}$$

Without loss of generality we assume

$$k_1^2 > k_2^2. \tag{7.7}$$

In this case by virtue of (7.5), (7.6)

$$k_1^2 - k_2^2 \geqslant 2\sqrt{b}. \tag{7.8}$$

One can show that $k_1^2 > 0$ (see the Appendix); in what follows we assume that k_2^2 is also positive† and therefore using (7.4*b*) equations (7.3*a*) are reduced to the system

$$J_2(k_1 a) + k_1 J_1(k_1 a)\left[\frac{M(U,a)}{b}\gamma_2 - N(U,a)\right] = 0, \tag{7.9a}$$

$$J_2(k_2 a) + k_2 J_1(k_2 a)\left[\frac{M(U,a)}{b}\gamma_1 - N(U,a)\right] = 0. \tag{7.9b}$$

Here γ_1, γ_2 is one of the pairs (7.5), (7.6). The pairs (7.9), (7.5) and (7.9), (7.6) will be referred to as cases 1 and 2 respectively.

† We cannot prove rigorously that $k_2^2 > 0$ in general case but analysis of the opposite case $k_2^2 < 0$ for particular values of the parameters U, a shows that the solution does not exist.

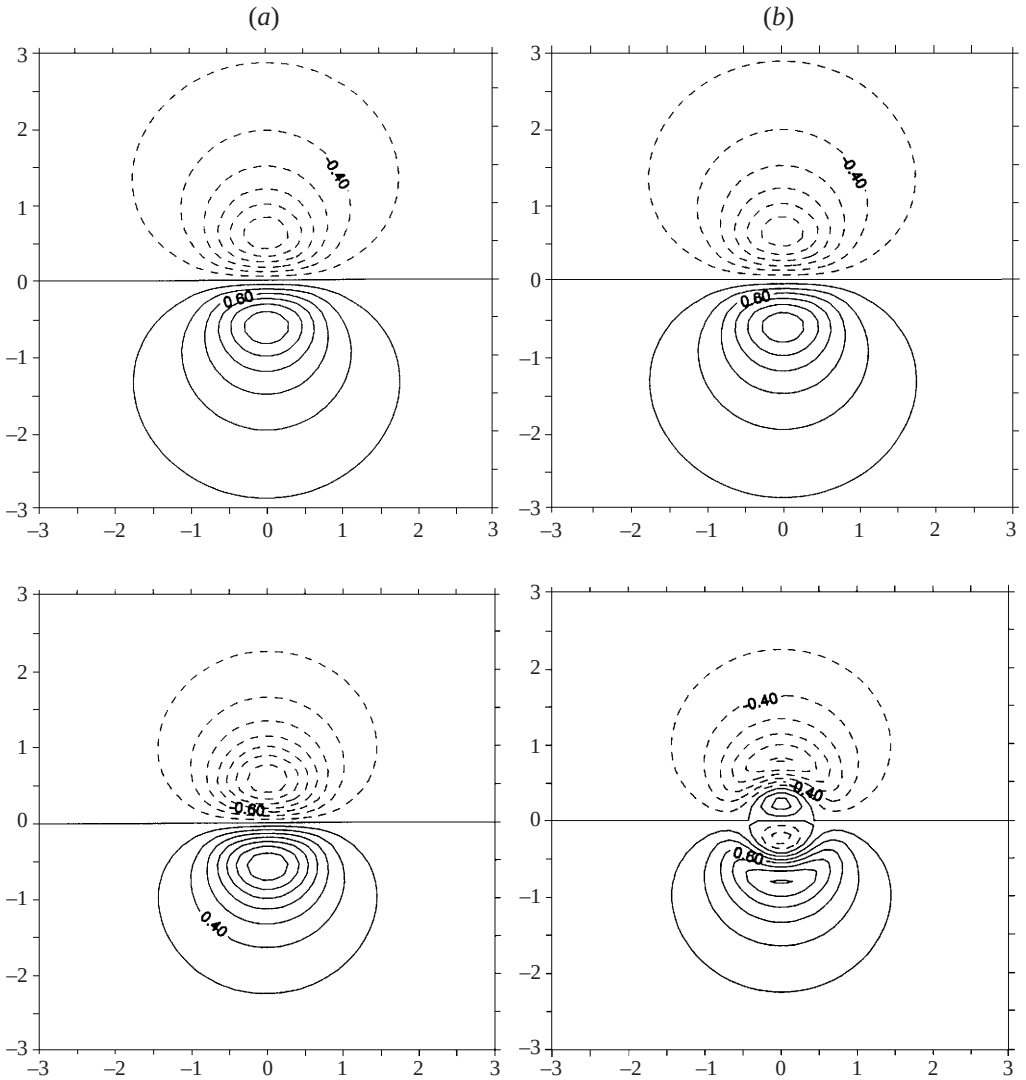

FIGURE 7. Modon with positive translation speed. Case 1. The dipole streamlines in the upper (top) and lower (bottom) layers for the lowest (*a*) and the second (*b*) pairs of the parameters k_1, k_2. $U = a = 1$, $b = 1$.

Given U, a equations (7.9) are curves on the plane k_1, k_2. In case 1 these curves are show in figure 6; the intersection points correspond to the roots k_1, k_2. (Note that the results in figures 6–11 are obtained using the internal Rossby scale, $L = \sqrt{g'\bar{h}/f_0}$, $\bar{h} = \bar{h}_1\bar{h}_2/(\bar{h}_1 + \bar{h}_2)$, instead of the length scale (2.3).) The dipole streamfunctions are represented in figures 7, 8 for $b = 1$ and $b = 4$, respectively. For the first roots $k_1^{(1)}$, $k_2^{(1)}$ the streamfunctions are simple dipoles in both layers; for the other roots the dipole structure is more complicated. Note that the dipole streamfunctions depend very weakly on the depth ratio b.

The coefficients in (4.16), (5.5) determining the rider component are also found from the conditions at the separating streamline (5.8); after some algebra

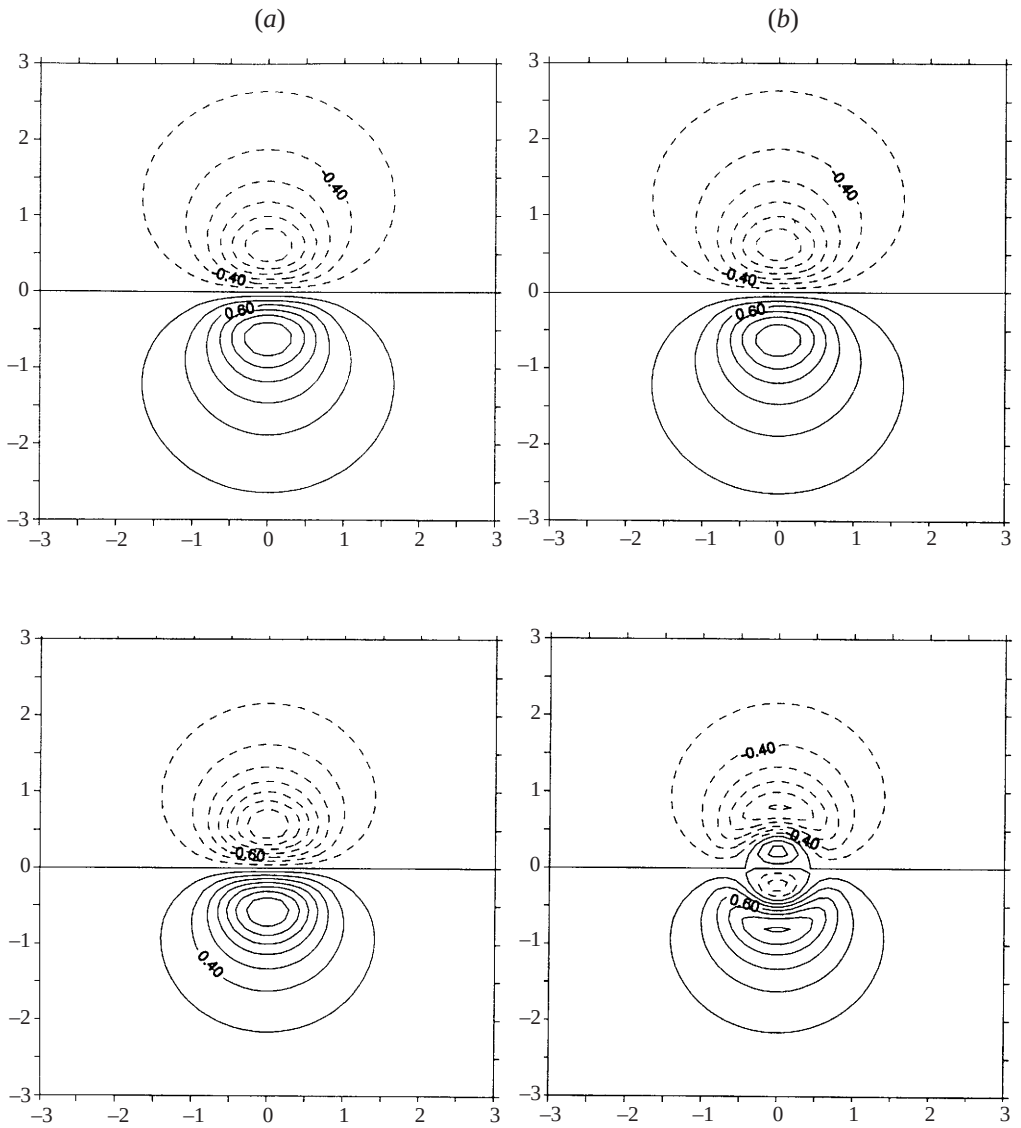

FIGURE 8. As figure 7 but for $b = 4$.

we have

$$A_{j0} = \frac{1}{(\alpha_2 - \alpha_1)k_j J_1(k_j a)}[p_1(\alpha_2 - \gamma_j)C_{10}K_1(p_1 a) + p_2(\gamma_j - \alpha_1)C_{20}K_1(p_2 a)], \qquad (7.10a)$$

$$\frac{Q_1 + \gamma_j Q_2}{k_j^2} = \frac{1}{(\alpha_2 - \alpha_1)}[(\alpha_2 - \gamma_j)C_{10}K_0(p_1 a) + (\gamma_j - \alpha_1)C_{20}K_0(p_2 a)] - A_{j0}J_0(k_j a). \qquad (7.10b)$$

Here the coefficients C_{10}, C_{20} are arbitrary.

Using (4.15), (4.16), (5.5), (5.7), and (7.10) one can calculate the rider streamfunction. The radial profiles of the streamfunction in the layers are shown in figure 9. We see

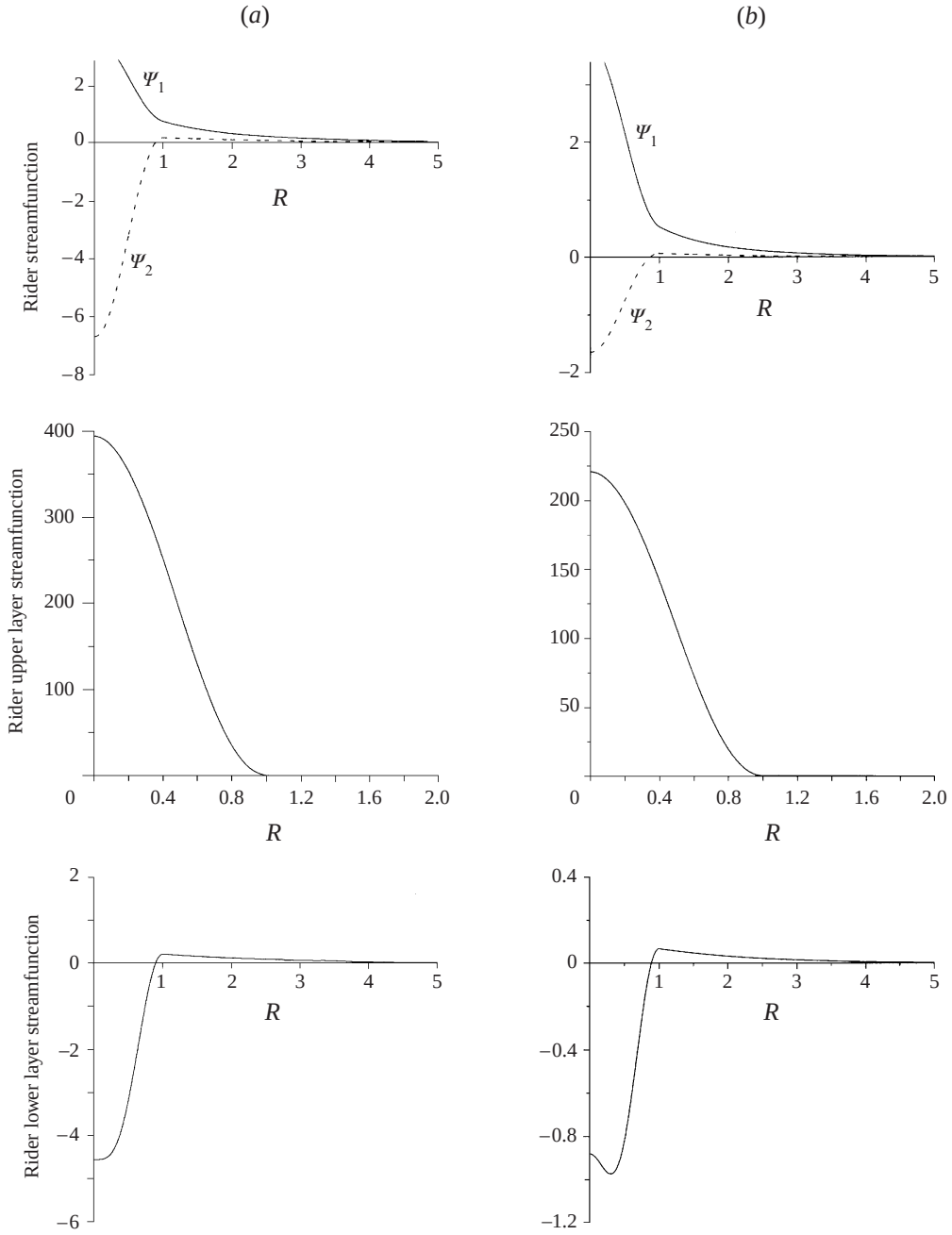

FIGURE 9. Modon with positive translation speed. Case 1. The radial profiles of the rider streamfunctions for the first (upper panels, lower layer streamfunction is shown by dashed line) and the second (middle and bottom panels) pairs of the parameters k_1, k_2: $U = a = 1$, $C_{10} = C_{20} = 1$. (*a*) $b = 1$, (*b*) $b = 4$.

that the upper-layer rider streamfunction is a monopole, whereas in the lower layer the streamfunction changes its sign to meet the condition (4.17*a*) of zero angular momentum. Note that the upper and lower vortices are counter-rotating in the modon core (interior domain). For the first root the amplitudes of these vortices

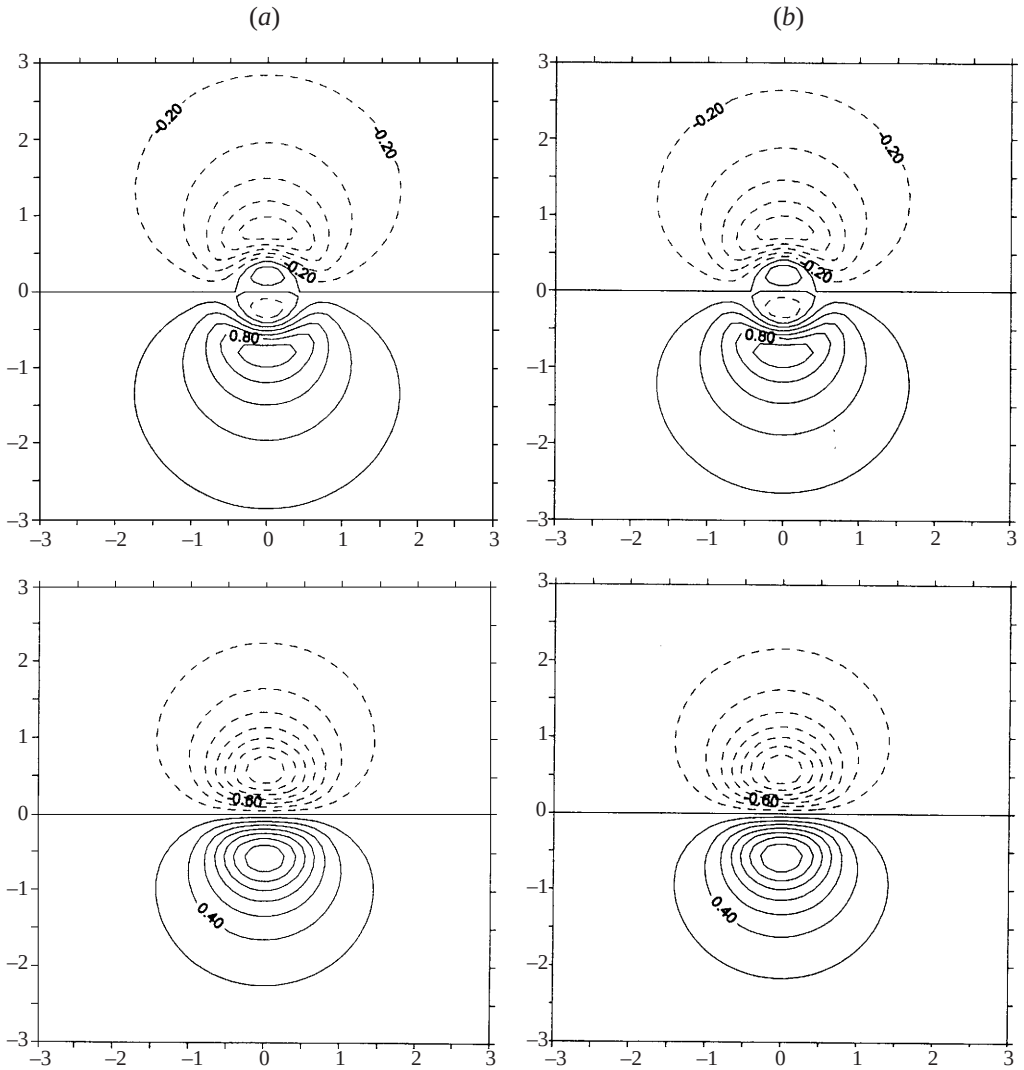

FIGURE 10. Modon with positive translation speed. Case 2. The dipole streamlines in the upper (top) and lower (bottom) layers for the first pairs of the parameters k_1, k_2; $U = a = 1$. (*a*) $b = 1$, (*b*) $b = 4$.

are comparable, for the second root the rider is confined mainly to the upper-layer interior domain.

Analogous results for case 2 are given in figures 10 and 11. The dipole structure is complicated even for the first root: the upper-layer streamfunction consists of four vortices. The riders are again confined mainly to the upper-layer interior domain but the streamfunction changes its sign in both layers. Contrary to the previous case the upper and lower vortices in riders are co-rotating in the modon core.

Note that riders with zero net angular momentum constructed for the barotropic modons on the beta-plane have a discontinuity in radial vorticity at the separating streamline and they were demonstrated numerically to be unstable (Swenson 1987). However, it was found by Kizner (1997) that in stratified fluid riders with a continuous

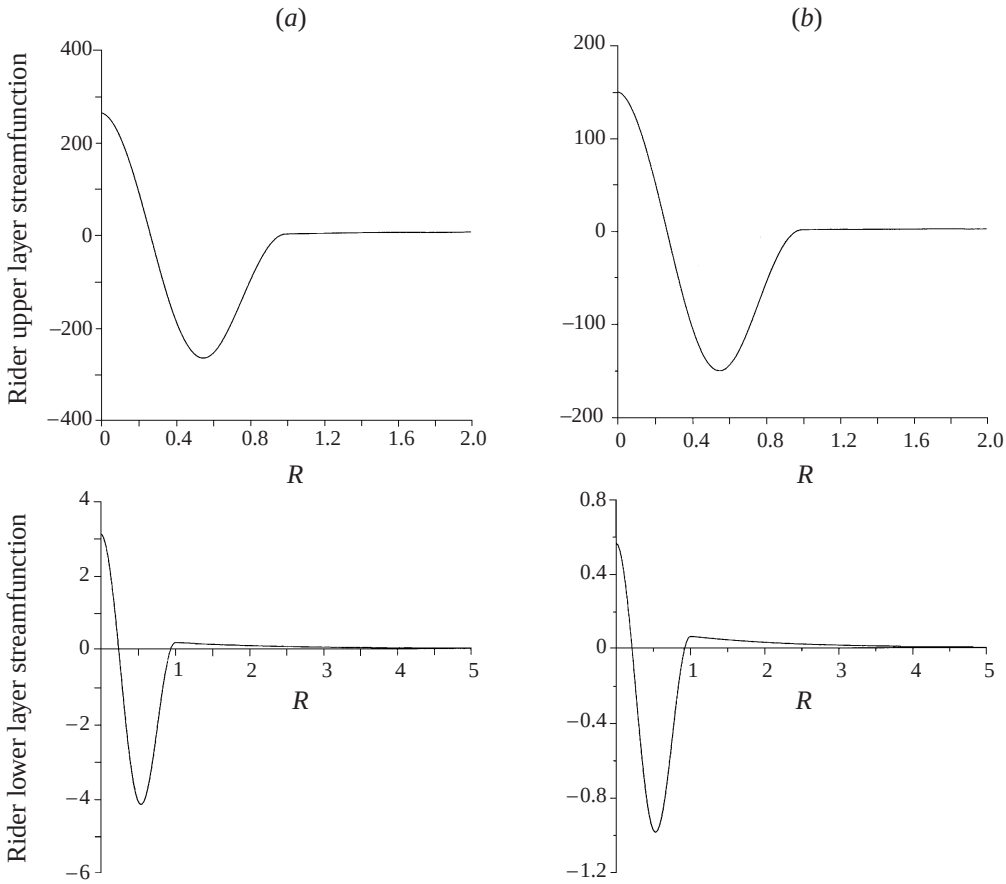

FIGURE 11. Modon with positive translation speed. Case 2. The radial profiles of the rider streamfunctions for the first pair of the parameters k_1, k_2; $U = a = 1$, $C_{10} = C_{20} = 1$. (*a*) $b = 1$, (*b*) $b = 4$.

vorticity profile exist. Numerical investigation of these riders shows that they can be remarkably stable (Z. I. Kizner 2000, private communication). The question of whether the riders with non-zero angular momentum presented here are stable is a subject of future studies.

8. Relations to other modon solutions

To clarify the cooperative effects of the stratification and topography on the BTM dynamics and relations to other modon solutions we consider how the present modon solutions behave in the limits of infinite ($b \to 0$) or zero ($b \to \infty$) upper-layer depth.

In the first case, the upper-layer equation (2.5*a*) is reduced to the equation for two-dimensional non-rotating fluid which does not possess localized solutions. Therefore, in the limit of infinite upper-layer depth the localized solutions may exist only if the upper layer is at rest. Then (2.5*b*) describes the equivalent-barotropic model on the topographic beta-plane which allows well-known modon solutions (e.g. Larichev & Reznik 1976; FLMR).

For the BTM solutions with negative translation speed considered in § 6, $-1 < U < 0$, and they do not tend to the equivalent-barotropic solutions with $U < -1$

because we assume that there is no interior domain in the lower layer. Rather they become non-localized because for the exterior field $p_2 \to 0$ when $b \to 0$ as seen from (6.9).

For the BTM solutions with positive translation speed considered in § 7, the interior domain exists in each layer. One can see from (4.7) that $p_1 \to 0$, and $p_2^2 \to 1 + 1/U$. Analysis of the dispersion relations (7.3)–(7.5) shows that the upper-layer streamfunction Ψ_1 tends to the non-localized Lamb's dipole which is proportional to $r^{-1} \sin\theta$ in the exterior domain. The lower-layer limiting state can be represented as a linear combination of the Lamb dipole, equivalent-barotropic modon, and a rather complicated field confined to the interior domain. Thus, the limiting BTM solutions for $b \to 0$ does not tend to any localized solutions of the corresponding limiting equations.

Similar behaviour is found in another limit of zero upper-layer depth ($b \to \infty$). The BTM solutions with negative translation speed also degenerate because their maximum size tends to zero as seen from (6.12). For the BTM solutions with positive translation speed, $p_1^2 \to 1/U$ and $p_2 \to \infty$, so that in this limit the first exterior mode corresponds to eastward propagating modon solutions for barotropic fluid while the second exterior mode vanishes. The dispersion relations (7.3)–(7.5) show that if k_2 is $O(1)$, then $k_1 \gg 1$. Correspondingly, the modon interior consists of the smooth component T_2 and rapidly oscillating component T_1.

In summary, we see that the BTM solutions with negative translation speed and no interior domain in lower layer cease to exist at both limits, i.e. they result from cooperative effects of stratification and topography. The BTM solutions with positive translation speed can be considered as a generalization of eastward-propagating well-localized modons either for barotropic or equivalent-barotropic models. Their new feature of non-zero net angular momentum is also a result of cooperative effects of stratification and topography.

9. Summary and conclusion

We have investigated the cooperative effect of stratification and bottom topography on modon dynamics using the model of a uniformly rotating two-layer ocean with a sloping bottom. The general properties of the BTM were studied and the exact solutions for the modons with piecewise-linear dependence of the potential vorticity on the streamfunction were given and analysed.

Two results are particularly important. The first result is that the BTM in a stratified ocean is able to move with a speed within the range of the phase velocities of linear topographic waves. The lack of resonant radiation in this case is conditioned by the orthogonality of the streamfunction field in the modon exterior to the corresponding field of the linear topographic wave propagating with the modon translation speed. At the same time the streamfunction in the modon core (interior domain) is not orthogonal to the linear wave streamfunction, i.e. the modon core 'contains' the resonant mode. One can say that the nonlinearity prohibits the radiation due to this mode. A solution with similar properties also exists in a two-layer ocean of constant depth on the beta-plane. This is the Rossby modon with purely baroclinic exterior found in FLMR.

This effect broadens the range of modon translation speeds and can be useful when modelling blocking events in the Earth's atmosphere. McWilliams (1980) pointed out that one of the impediments to the use of barotropic modons as such a model is related to the modon's inability to drift westward with a speed within the range of

the Rossby wave phase speeds. The solution presented shows that this shortcoming can be avoided if the model of blocking events incorporates the stratification and the bottom topography. Note that the planetary beta-effect plays dominant role in the atmosphere and it should be taken into account together with the topography to allow applicability of the BTM solutions to the atmospheric coherent structures. Our work in this direction is in progress and the results will be reported elsewhere.

The second important result making the BTMs significantly different from their beta-plane analogues (see Flierl, Stern & Whitehead 1983) is that the total angular momentum of the vortex over a sloping bottom can be non-zero. More exactly, the integral angular momentum in the bottom layer should be zero; the upper layer angular momentum can be non-zero. This feature provides for the existence of modons carrying axisymmetric riders representing intense monopolar vortices confined to the upper layer. As the rider amplitude is arbitrary the dipole component can be 'masked' and the composed modon looks like a monopole. This property is especially interesting since the majority of the observed long-lived vortices are monopoles.

The authors thank Professor Z. Kizner (BIU) for a helpful discussions and anonymous reviewers for valuable remarks. This study was supported by Russian Foundation for Basic Research Grant #99-05-64841 and the USA National Science Foundation Grant ATM-9905209

Appendix

Using (7.3*a*), (7.4*b*) one can show that

$$[R_1(k_1,a)-N][R_2(k_2,a)-N]=\frac{M^2}{b},\quad R_j(k_j,a)=\frac{J_2(k_ja)}{|k_j|J_1(k_ja)}. \tag{A 1}$$

By virtue of (4.8*b*, *c*)

$$1+\alpha_2<0\quad\text{for}\quad U>0 \tag{A 2}$$

whence

$$N<0. \tag{A 3}$$

Then at least one of the quantities $R_1, R_2(k_1^2, k_2^2)$ should be negative (positive) and therefore (see (7.7))

$$k_1^2>0. \tag{A 4}$$

REFERENCES

Berestov, A. L. 1979 Solitary Rossby waves. *Izv. Akad. Nauk SSSR. Atmos. Ocean Phys.* **15**, 648–654.

Carnevale, G. F., Briscolini, M., Purini, R. & Vallis, G. K. 1988*a* Numerical experiments on modon stability to topographic perturbations. *Phys. Fluids* **31**, 2562–2566.

Carnevale, G. F., Vallis, G. K., Purini, R. & Briscolini, M. 1988*b* Propagation of barotropic modons over topography. *Geophys. Astrophys. Fluid Dyn.* **41**, 41–101.

Flierl, G. R. 1987 Isolated eddy models in geophysics. *Ann. Rev. Fluid Mech.* **19**, 493–530.

Flierl, G. R., Larichev, V. D., McWilliams, J. C. & Reznik, G. M. 1980 The dynamics of baroclinic and barotropic solitary eddies. *Dyn. Atmos. Oceans* **5**, 1–41 (referred to herein as FLMR).

Flierl, G. R., Stern, M. E. & Whitehead, J. A. 1983 The physical significance of modons: Laboratory experiments and general integral constraints. *Dyn. Atmos. Oceans* **7**, 233–263.

Kamenkovich, V. M., Koshlyakov, M. N. & Monin, A. S. 1986 *Synoptic Eddies in the Ocean.* Reidel, Dordrecht.

Kizner, Z. I. 1984 Rossby solitons with axisymmetrical baroclinic modes. *Dokl. Akad. Nauk SSSR* **275**, 1495–1498.

Kizner, Z. I. 1986 Strongly non-linear solitary Rossby waves. *Oceanology* **26**, 382–388.

Kizner, Z. I. 1988 To the theory of inthrathermocline eddies. *Dokl. Akad. Nauk SSSR* **300**, 453–457.

Kizner, Z. I. 1997 Solitary Rossby waves with baroclinic modes. *J. Mar. Res.* **55**, 671–685.

Larichev, V. D. & Reznik, G. M. 1976 On the two-dimensional solitary Rossby waves. *Dokl. Akad. Nauk SSSR* **231**, 1077–1079.

McWilliams, J. C. 1980 An application of equivalent modons to atmospheric blocking. *Dyn. Atmos. Oceans* **5**, 43–66.

Mied, R. P., Kirwan, A. D., Jr. & Lindemann, G. J. 1992 Rotating Modons over isolated topographic features. *J. Phys. Oceanogr.* **22**, 1569–1582.

Nezlin, M. V. & Sutyrin, G. G. 1994 Problems of simulation of large, long-lived vortices in the atmospheres of the giant planets (Jupiter, Saturn, Neptune). *Surveys in Geophys.* **15**, 63–99.

Pakyri, A. & Nycander, J. 1996 Steady two-layer vortices on the beta-plane. *Dyn. Atmos. Oceans* **25**, 67–86.

Reznik, G. M. 1985 An exact solution for the two-dimensional topographic solitary Rossby wave. *Dokl. Akad. Nauk SSSR* **285**, 981–985 (in Russian).

Reznik, G. M. 1999 On generation of the sub-surface motion in stratified ocean with sloped bottom. *Oceanology* **39**, 325–327 (in Russian).

Reznik, G. M. & Sutyrin, G. G. 2000 General properties of baroclinic modons over topography. *Proc. IUTAM Symp. on Advances in Mathematical Modelling of Atmosphere and Ocean Dynamics, University of Limerick, Ireland* (ed. F. Hodnett).

Stern, M. E. 1975 Minimal properties of planetary eddies. *J. Mar. Res.* **33**, 1–13.

Swaters, G. E. 1986 Barotropic modon propagation over slowly varying topography. *Geophys. Astrophys. Fluid Dyn.* **36**, 85–113.

Swenson, M. 1987 Instability of equivalent-barotropic riders. *J. Phys. Oceanogr.* **17**, 492–506.